Available online at www.eccomasproceedia.org
Eccomas Proceedia COMPDYN (2025) 754- 765

ECCOMAS Proceedia

COMPDYN 2025
10th ECCOMAS Thematic Conference on
Computational Methods in Structural Dynamics and Earthquake Engineering
M. Papadrakakis, M. Fragiadakis (eds.)
Rhodes Island, Greece, 15-18 June 2025

APPLIED ELEMENT MODELLING OF MASONRY ARCHES STRENGTHENED WITH FRCM

Nicola Scattarreggia[1,2], Mattia Calò[1,2], Ricardo Monteiro[1,2]

[1] Scuola Universitaria Superiore IUSS Pavia
Piazza della Vittoria 15, 27100, Pavia, Italy
{nicola.scattarreggia, mattia.calo, ricardo.monteiro}@iusspavia.it

[2] RESISK srl
V.le Col di Lana 12/A, 20136, Milan, Italy
{nicola.scattarreggia, mattia.calo, ricardo.monteiro}@resisk.com

Abstract

This paper describes a discrete element numerical model of masonry arches validated through a series of experimental tests, developed within an Applied Element Method (AEM) framework. The study assesses the effectiveness of strengthening masonry arches using a fibre-reinforced cementitious mortar (FRCM) coating (Planitop Intonaco Armato®) applied to the extrados. Following the validation of the AEM-based numerical model with experimental results of both unreinforced and strengthened (using FRCM in combination with polybenzoxazole (PBO) fabric) masonry arches, the model has been further employed to analyse the use of the FRCM material Planitop Intonaco Armato. The strengthening measure was modelled using a simplified grid-based approach, representing the retrofit as a single layer of springs at the extrados, an approach initially validated against experimental tests. As result, numerical analyses were conducted to evaluate the impact of the FRCM strengthening system on load-carrying capacity, post-peak behaviour, and failure mechanisms. While previous validation analyses indicated that the AEM framework accurately reproduces the experimental performance of URM arches and effectively predicts the enhancement provided by the retrofit, the findings underscore the potential of the FRCM Planitop Intonaco Armato as a viable alternative strengthening solution. Preliminary sensitivity analyses revealed its effectiveness is greater when the unreinforced masonry arch has weaker material properties, but its beneficial impact diminishes as the material properties of the arches improve.

Keywords: strengthening, masonry, arches, FRCM composite, Applied Element Method.

doi: 10.7712/120125.12688.26019

1 INTRODUCTION

Historical masonry structures represent a significant part of the world's cultural heritage, embodying both architectural and historical value. However, many of these structures are vulnerable to seismic actions due to material degradation, ageing, and original design according to the knowledge of those times. Therefore, their structural assessment and potential retrofitting are critical to ensure their long-term preservation and safety. Seismic evaluation of these structures requires advanced numerical techniques capable of capturing their complex failure mechanisms. This challenge is further exacerbated by the intricate geometries often found in historical constructions, such as arches, vaults, and domes, which exhibit highly nonlinear behaviour under seismic loads. These structural forms introduce additional complexities related to force redistribution, thrust mechanisms, and multi-directional interactions, requiring modelling approaches that can accurately reproduce their discrete and anisotropic nature (as also described in, e.g., [1, 2, 3]).

Traditional continuum-based approaches, such as the Finite Element Method (FEM), often struggle to accurately model the discrete nature of masonry, which consists of individual units (e.g., bricks or stones) and mortar joints. These methods typically require homogenisation techniques or predefined crack paths, limiting their ability to fully capture localised damage, crack initiation, and propagation under dynamic loading (see e.g. [3, 4, 5]). Conversely, discontinuum approaches [6] provide a significant advantage in this context, as they enable a more detailed representation of contact interactions and failure modes, including localised crushing, sliding, large displacement effects, and explicit damage propagation until failure.

Within such a context, the Distinct Element Method (DEM) [7] has proven to be a powerful tool for simulating the response of complex masonry structures, thanks to its ability to explicitly represent their discontinuous nature. This approach allows for accurate modelling of individual units, large displacements, joint opening and closure, and even complete block separation. Numerous studies have demonstrated the effectiveness of DEM in predicting both static and dynamic responses of masonry, including in-plane and out-of-plane behaviour of unreinforced walls, as well as the performance of retrofitted structures (see e.g. [8, 9, 10]). Furthermore, DEM has been successfully applied to analyse more intricate masonry systems, such as vaults, domes, arch bridges, and spires (see e.g. [11, 12]). However, despite its advantages, DEM requires a significant computational effort, making it highly demanding in terms of processing time.

In contrast, the Applied Element Method (AEM) [13] presents itself as an efficient and promising alternative. AEM retains the capability to simulate large displacements, joint interactions, and even collapse mechanisms, while significantly reducing computational costs. Its formulation enables an effective balance between accuracy and efficiency, making it a compelling choice for large-scale structural analyses and real-time applications. It has been proven to be particularly effective in simulating the nonlinear behaviour of not only reinforced concrete and steel structures ([14, 15]), but also masonry structures [16, 17, 18]. For instance, Davis et al. [19] analysed the response of historical masonry churches under seismic loads through AEM-based models, including the modelling of their progressive damage and collapse mechanisms, encouraging the use of AEM to assess the structural performance of retrofitted historical structures.

The present work numerically validates an experimental testing campaign [20] and the corresponding AEM modelling strategy focusing on the structural performance of masonry arches externally reinforced with a cementitious matrix composite incorporating polybenzoxazole (PBO) fabric. The primary investigated aspects include load-bearing capacity, post-peak behaviour, and failure mechanisms. The study seeks to enhance the predictive capability of AEM-based simulations for masonry arches strengthened with composite materials.

Following the validation of the AEM-based numerical model with experimental results for both unreinforced and strengthened masonry arches (using FRCM with PBO fabric), further analyses were conducted to assess the effectiveness of the FRCM material *Planitop Intonaco Armato* [21]. Two modelling approaches were employed: a standard explicit method, representing the coating as a virtual assembly of rigid units, and a simplified grid-based approach using a single layer of springs at the extrados. Once the simplified grid-based approach was validated, it was then used to analyse the arches strengthened using the FRCM material Planitop *Intonaco Armato.* Numerical simulations evaluated the impact of the strengthening system on load-carrying capacity, post-peak behaviour, and failure mechanisms, along with sensitivity analyses to explore the influence of masonry properties on the retrofit's effectiveness.

2 DESCRIPTION OT THE EXPERIMENTALLY TESTED ARCHES

To investigate the structural behaviour of reinforced masonry arches under out-of-plane loading, the experimental tests carried out by Alecci et al. [20] have been considered. The tests investigated the structural behaviour of scaled masonry arches strengthened with PBO-FRCM composite at the extrados (i.e. specimens named 1-2/PeS). The tested arches were built at a 1:2 scale, with a span of 1500 mm, an intrados radius of 866 mm, an extrados radius of 961 mm, and a rise of 432.5 mm. Each arch had a uniform cross-section of 95 × 95 mm², constructed using bricks measuring 95 × 46 × 21 mm³ with mortar joints of 5 mm thickness.

The strengthening intervention of the considered specimens involved applying a PBO-FRCM composite layer along the extrados. The PBO textile was then placed over an initial 3 mm thick cementitious matrix layer, and a second matrix layer was applied, resulting in a final composite thickness of approximately 6 mm. The reinforcement covered the entire extrados width of 95 mm with a fibre cross-sectional area of 1.33 mm².

A vertical force was applied at a quarter-span (375 mm from the left abutment) through a 20 mm thick steel plate. The applied load was recorded using a 10 kN tension/compression load cell, while the corresponding vertical displacements were recorded.

The masonry used for constructing the arches was mechanically characterised through compression and shear tests. Additionally, triplet tests were conducted to determine both cohesion and friction coefficient.

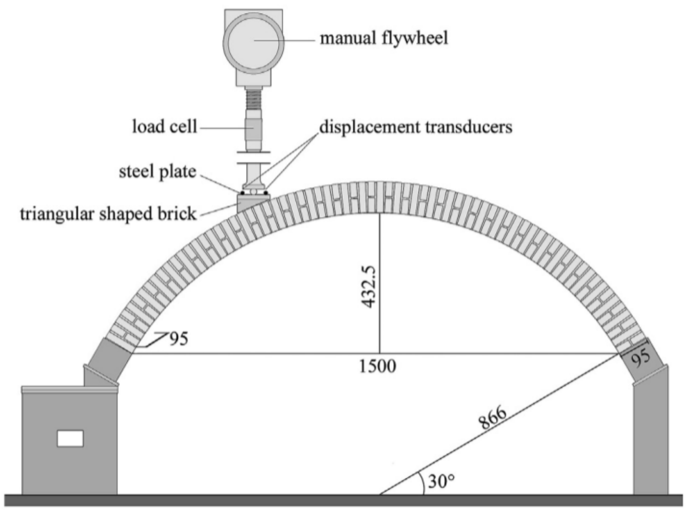

Figure 1: Test set-up for the tested arches (Adapted from [20]).

Regarding the strengthened arches, the employed FRCM composite consisted of a balanced bidirectional PBO fabric embedded in an inorganic, pozzolanic cement-based mortar matrix. The mechanical properties of the PBO-FRCM composite were initially assessed by characterising its constituent materials, including the cementitious mortar and the PBO fabric. The available material test results from [20] were used as reference to develop the numerical model, as described in the following sections.

3 NUMERICAL MODELLING

The following subsections outline the modelling approach and strategies used to analyse the response of the masonry arch in both its as-built and strengthened configurations. The description begins with the as-built model, followed by an overview of the numerical methods employed to integrate the strengthening system.

3.1 As-built arch modelling

The Applied Element Method (AEM) was used for the numerical models using the commercial software Extreme Loading for Structures (ELS) [22]. According to the AEM formulation, a structure is discretised as a virtual assembly of rigid units, which carry only the system's mass and damping, connected by linear and nonlinear springs that feature the material properties. This allows for the simplified micro-modelling of masonry, where a wall segment is represented by fully rigid or deformable units connected by zero-thickness mortar joints. The method inherently accounts for contact interactions and dynamic effects, enabling a seamless transition between continuum and discrete numerical representations. Further details on the theoretical background of AEM can be found in [13].

In this study, each masonry unit in the arch was represented as a single rigid element (see Figure 2). This choice was driven by two main considerations: first, to reproduce cracking patterns occurring only along the vertical joints; second, to avoid excessive computational costs associated with further sub-discretisation of bricks. While this assumption prevents the simulation of intra-unit failures, such as brick crushing, this limitation was deemed acceptable as no such mechanisms were observed during the experimental tests. The interface between elements was carefully calibrated to reproduce the macroscopic behaviour of masonry. Specifically, a nonlinear constitutive model was implemented, featuring a parabolic response in compression, a linear response in tension up to peak strength and ultimate strain, and a cohesive-frictional behaviour in shear. Based on the testing results from [20], the adopted material properties for masonry are reported in Table 1.

Parameter	Masonry	FRCM	PBO
ρ [kg/m^3]	1800	1800	1560
E [MPa]	2000	2800	2.2E+05
G [MPa]	800	1100	8E+04
ν [-]	0.25	0.2	0
f_u [MPa]	8	20	0
f_t [MPa]	0.50	4.8	3500
f_{v0} [MPa]	0.26	4.8	3500
μ [-]	0.6	0.6	0.8

ρ: material density; E: young modulus; G: shear modulus; ν: Poisson coefficient; f_u: ultimate compression strength; f_t: ultimate tensile strength; f_{v0}: cohesion; μ: friction coefficient.

Table 1: Materials properties adopted in the AEM-based numerical model.

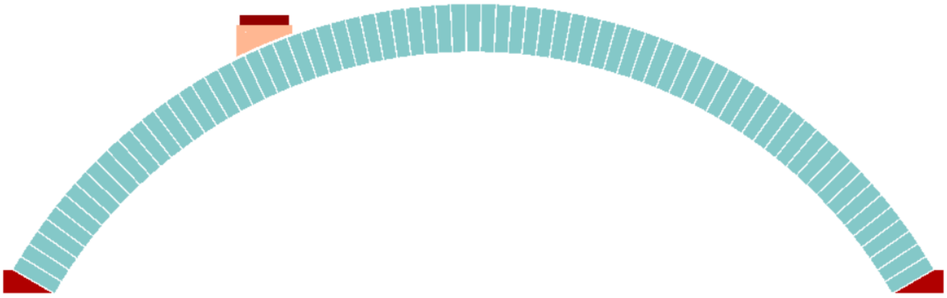

Figure 2: AEM modelling of the as-built masonry arch.

3.2 PBO-FRCM strengthening modelling

Two distinct modelling strategies have been tested within the discrete modelling environment to represent the strengthening system. The explicit modelling strategy represents the PBO reinforcement and mortar layers as separate geometrical entities. In this case, the geometry of the mortar layer is explicitly modelled with a thickness of 6 mm, positioned within the masonry structure as shown in Figure 3a. The reinforcement mesh is placed at the mid-thickness of the mortar layer (i.e., at 3 mm from the extrados of the arch). It is only represented in the longitudinal direction, as the transverse direction is not necessary given the in-plane loading conditions. To ensure consistency with the surrounding rigid blocks, the mesh size of the mortar layer needs to be at least equal to the width of the neighbouring rigid blocks, preventing numerical interference with the fracture mechanisms of the masonry structure. However, due to the explicit discretisation of the mortar, this approach significantly increases the number of elements within the discrete environment, resulting in a higher computational burden due to the increase of the system's degrees of freedom. Nevertheless, this method provides a detailed and accurate representation of the reinforcement and mortar layers, maintains a direct physical interpretation of material interactions, and allows for straightforward parameter adjustments and refinement.

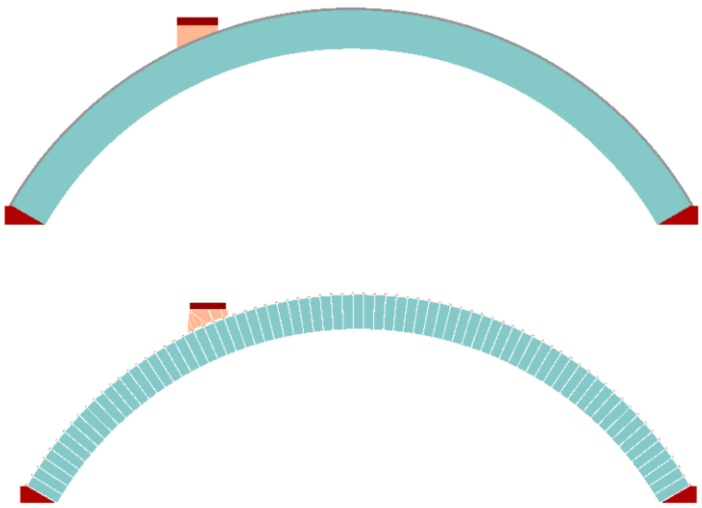

Figure 3: AEM modelling of the arch using the (a) explicit and (b) equivalent modelling of PBO-FRCM strengthening measure.

The alternative modelling approach simplifies the representation of the PBO reinforcement and mortar layers by using an equivalent lattice representation. Instead of explicitly modelling the mortar (as for the explicit version), this method introduces reinforcement bars that approximate its behaviour similarly to the PBO reinforcement modelling, ensuring that their total cross-sectional area corresponds to the actual mortar thickness over a width of 95 mm. A key characteristic of this modelling approach is that both the reinforcement and the mortar are positioned right above the extrados of the masonry arch to generate the springs between blocks. This introduces additional normal springs on one side of the arch, as illustrated in Figure 3. The increased number of springs at the interface slightly raises the computational cost due to the additional contact calculations. However, the stiffness matrix size remains unchanged, as no additional structural elements are introduced. This permits to reduce the total number of elements in the model, thereby improving computational efficiency compared to the explicit approach, preserves key mechanical interactions through an equivalent representation, and provides flexibility in adjusting reinforcement and mortar characteristics without refining the mesh. On the other hand, it offers a less intuitive physical interpretation and requires careful calibration of equivalent material properties to ensure accuracy.

The adopted material properties for FRCM and PBO are reported in Table 1, again based on the testing results from [20].

4 RESULTS

4.1 Validation with experimental test: unstrengthen arches

Figure 4 presents the results in terms of vertical base reaction and mid-span displacement curves. Figure 5, in turn, compares the experimental and numerically obtained failure mechanisms. A good agreement was observed for a tensile strength value of 0.5 MPa, although the numerical model exhibits a slightly lower initial stiffness compared to the experimental response. The numerical sequence of hinge formation was the same as for the experimental test, and the final configuration is the one shown in Figure 5. Their position presents overall a good correspondence.

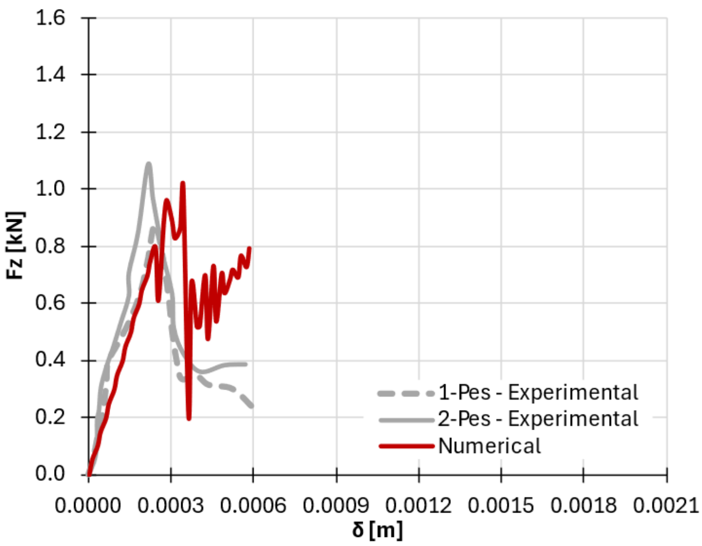

Figure 4: Comparison between the experimental and numerical curves in terms of vertical base reaction vs. mid-span vertical displacement for the as-built arch.

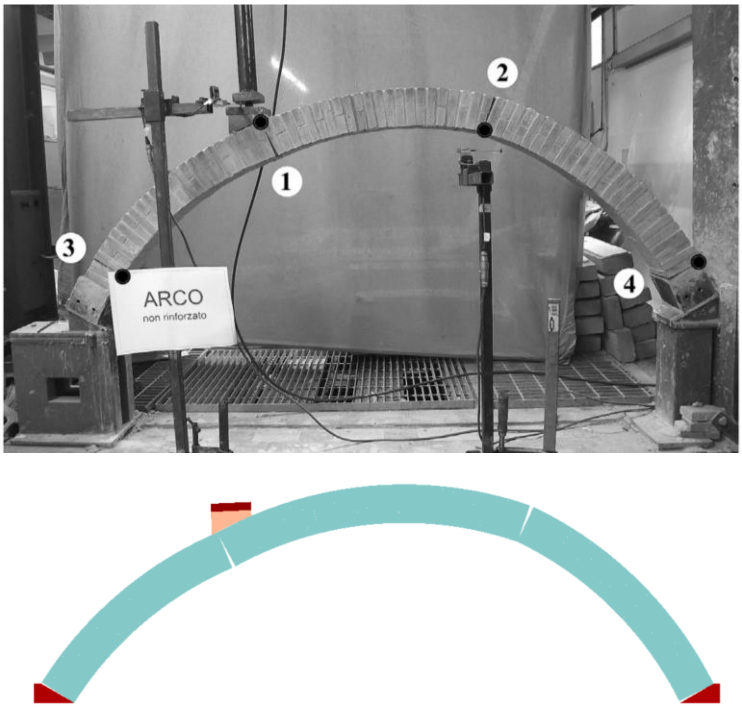

Figure 5: Comparison between the experimental (adapted from [20]) and numerical failure mechanisms (at the end of test) for the as-built arch.

4.2 Validation with experimental test: PBO-FRCM strengthened arches

The validation was conducted on the specimen reinforced at the extrados through the application of the PBO composite and FRCM mortar with a thickness of approximately 6 mm. In the experimental test, a plastic hinge developed first (beneath the steel plate), accompanied by the propagation of other cracks. The final failure occurred with the debonding of the strengthening system that ended up with the shear slip at the steel abutment (Figure 6). It cannot be ruled out that, had the slip been prevented, a higher load-bearing capacity could have been achieved, depending on the tensile strength of the extrados reinforcement. The failure mechanisms presented in Figure 7 indicate that both PBO-FRCM strengthening modelling strategies are aligned in their predictions.

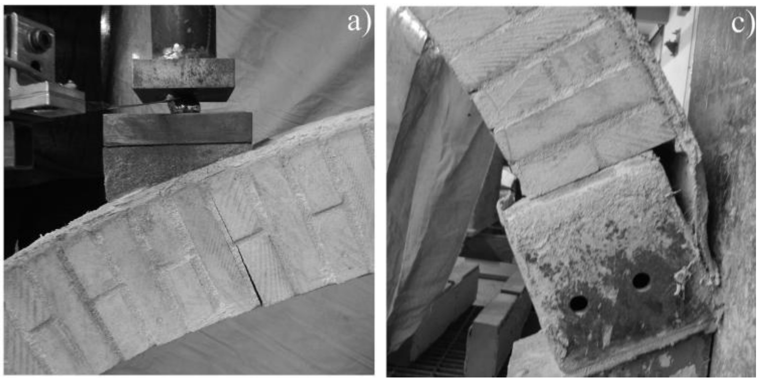

Figure 6: Observed first hinge formation and shear slip mechanism at failure in the PBO-FRCM-strengthened arch. (Adapted from [20]).

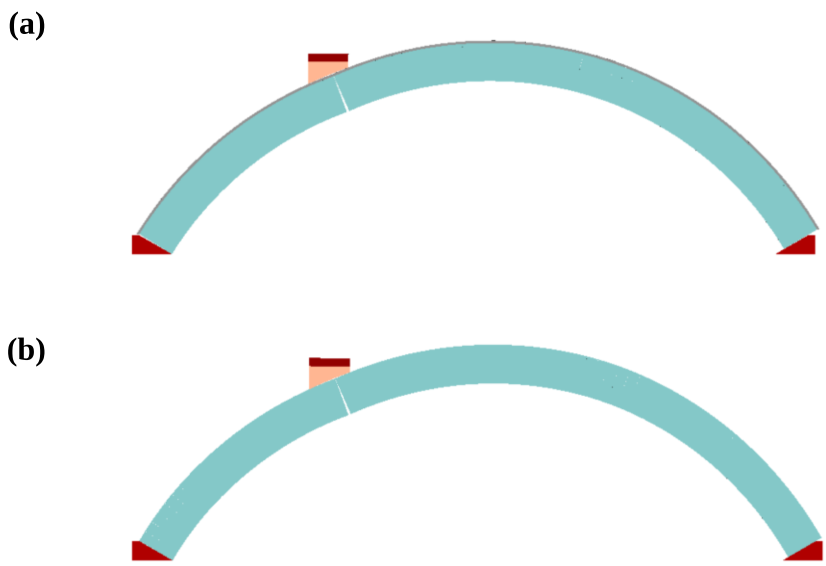

Figure 7: Numerical failure mechanism using the (a) explicit and (b) equivalent strengthening modelling of the mortar.

The comparison of push-down curves between the experimental and numerical results is shown in Figure 8. Both numerical models align closely with each other, in terms of initial stiffness, peak strength, and post-peak response. The first hinge at the intrados forms at approximately 3 kN in the numerical models, compared to around 3.5 kN in the experimental test. Following this, the response is primarily governed by shear slip and the complex resistance mechanism that develops at the right steel abutment at around 4 kN. While the peak resistance is consistent with the experimental results, differences are observed in terms of stiffness after the first hinge forms. Additionally, the residual peak strength is lower than that observed in the experimental test. Despite these differences, both models successfully capture the overall response, a notable achievement given the uncertainty involved in the complex shear slip failure mechanism that was observed.

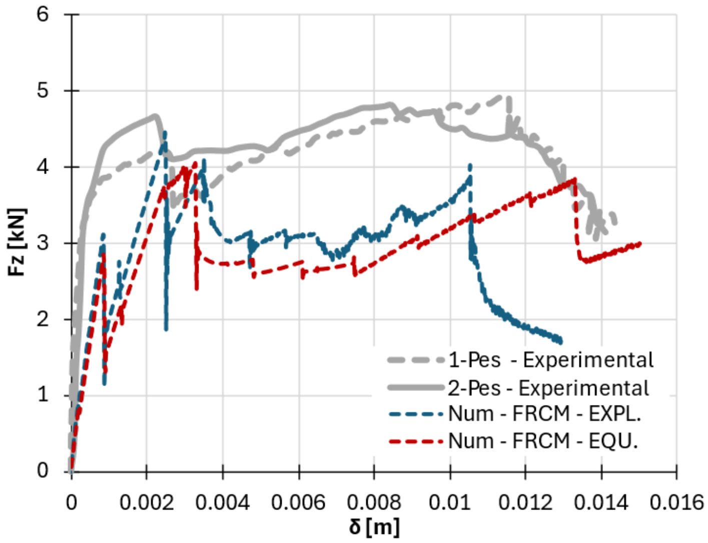

Figure 8: Comparison between the experimental and numerical curves of vertical base reaction vs. mid-span vertical displacement for the PBO-FRCM strengthened arches.

4.3 Arches strengthened with FRCM using *Planitop Intonaco Armato*

The same arch was used for a preliminary study on the response from strengthening with the sole introduction of FRCM. Specifically, the arch was strengthened with a 15 mm thick FRCM coating (*Planitop Intonaco Armato*®) applied to the extrados. According to the manufacturer's specifications [21] and additionally provided testing results, the adopted mortar features a tensile strength of 0.69 MPa, shear strength of 0.15 MPa, compressive strength of 23 MPa, and a Young's modulus of 8000 MPa. In addition to the masonry arch properties given in Section 4.1, the analysis has been conducted assuming also that the masonry in the as-built condition is relatively weak, allowing for an initial understanding of how the existing masonry properties affect the strengthening system effectiveness. The weak masonry was assigned the following reduced parameters: maximum compressive strength of 5.1 MPa, maximum tensile strength of 0.06 MPa, and cohesion of 0.18 MPa, thus very low tensile and shear resistance.

Based on the encouraging validation in Section 4.2, the equivalent modelling approach was applied for this preliminary study to model the FRCM strengthening. The results, shown in Figure 10, indicate that the introduction of the FRCM layer significantly enhances the peak strength of the as-built structure. For masonry with weak properties, the peak strength increased by approximately 400%, while for stronger masonry (as the one assumed in Sections 4.1 and 4.2), the increase was around 25%. Furthermore, the failure mechanism remained largely unchanged when compared to the original as-built structure, with only a slight shift in the hinge formation (on the left), as illustrated in Figure 11.

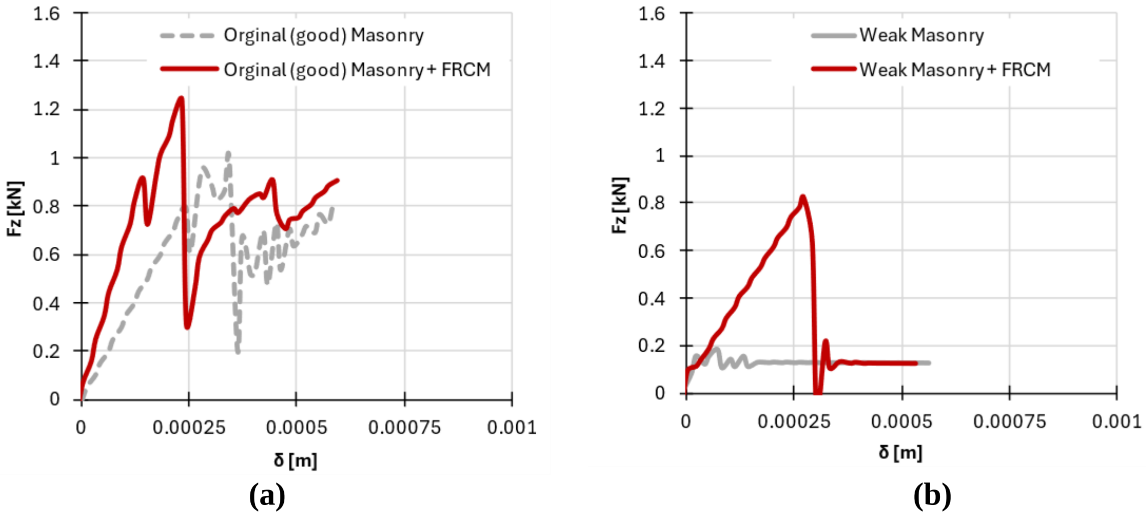

Figure 10: Numerical curves of vertical base reaction vs. mid-span vertical displacement for the FRCM strengthened arch with (a) original (good) masonry and (b) assumed weak masonry.

Figure 11: Numerical failure mechanism observed in the arch with weak masonry strengthened using FRCM (*Planitop Intonaco Armato*).

5 CONCLUSIONS

This study preliminarily assessed the effectiveness of an FRCM (*Planitop Intonaco Armato*®) strengthening system applied to masonry arches using a discrete element numerical model developed within an Applied Element Method (AEM) framework. The objective was to evaluate the impact of the reinforcement on load-carrying capacity and failure mechanisms, while also exploring computationally efficient modelling strategies for large-scale purposes.

The numerical models were initially validated against experimental tests conducted on both unreinforced and retrofitted masonry arches. The results confirmed that the AEM framework accurately reproduces the structural response of as-built arches and effectively captures the enhancement provided by the FRCM strengthening, particularly when used in combination with polybenzoxazole (PBO) fabric. The comparison between experimental and numerical results demonstrated a good agreement in terms of load-bearing capacity and overall response, supporting the reliability of a simplified modelling approach of FRCM mortar.

This approach, based on an equivalent grid of springs at the extrados, was calibrated against the explicit modelling technique, which represents the FRCM as an assembly of rigid elements. Indeed, the simplified approach successfully replicated the key mechanical behaviour observed in the detailed explicit model while significantly reducing computational costs, making it a practical alternative for parametric and large-scale analyses.

A sensitivity analysis was then conducted to examine the influence of the masonry arch's material properties on the effectiveness of the solely FRCM strengthening. The results indicated that the adopted strengthening system is most beneficial when applied to arches with weaker masonry, providing a notable increase in peak strength. Conversely, for stronger masonry, the adopted FRCM strengthening had a more limited impact, primarily serving as a supplementary enhancement rather than a transformative intervention.

Future research will expand these findings by exploring a broader range of geometries and loading conditions to further refine the modelling approach and optimise the application of FRCM strengthening systems in masonry structures.

REFERENCES

[1] D. Foti, V. Vacca, I. Facchini, DEM modeling and experimental analysis of the static behavior of a dry-joints masonry cross vaults. *Construction and Building Materials*, **170**, 111–20, 2028. DOI: 10.1016/j.conbuildmat.2018.02.202

[2] D. Malomo, M.J. DeJong, A. Penna, Influence of bond pattern on the in-plane behavior of URM piers. *International Journal of Architectural Heritage*, 15(10), 1492–511, 2021. DOI: 10.1080/15583058.2019.1702738

[3] A. Furiosi, N. Damiani, A. Penna, Structural Assessment of a Masonry Vault Using the Distinct Element Method, Milani, G., Ghiassi, B., *18th International Brick and Block Masonry Conference* (IB2MaC 2024). *Lecture Notes in Civil Engineering*, 613. https://doi.org/10.1007/978-3-031-73314-7_18

[4] D. Theodossopoulos, B.P. Sinha, A.S. Usmani, A.J. Macdonald, Assessment of the structural response of masonry cross vaults. *Strain* **38**, 119-127, 2002. DOI: 10.1046/j.0039- 2103.2002.00021.x

[5] E. Milani, G. Milani, A. Tralli, Limit analysis of masonry vaults by means of curved shell finite elements and homogenization. *International Journal of solids and structures* 45(20), 5258-5288, 2018. DOI: 10.1016/j.ijsolstr.2008.05.019

[6] D. Malomo, B. Pulatsu, Discontinuum models for the structural and seismic assessment of unreinforced masonry structures: a critical appraisal. *Structures* 62, 106108, 2024. DOI: 10.1016/j.istruc.2024.106108

[7] P.A. Cundall, A Computer Model for Simulating Progressive Large Scale Movements in Blocky Rock System. *Proceedings of the Symposium of the International Society of Rock Mechanics*, Nancy, France, 1971.

[8] J.V. Lemos, Discrete element modeling of masonry structures. *International Journal of Architectural Heritage* 1(2), 190-213, 2007. DOI: 10.1080/15583050601176868

[9] D. Malomo, M.J. DeJong, M-DEM simulation of seismic pounding between adjacent masonry structures. *Bulletin of Earthquake Engineering*, 1-26, 2022. DOI: 10.1007/s10518-022-01545-2.

[10] N. Damiani, M.J. DeJong, L. Albanesi, A. Penna, P. Morandi, Distinct element modeling of the in-plane response of a steel framed retrofit solution for URM structures. *Earthquake Engineering Structural Dynamic*, 52(10), 3030-3052, 2023. DOI: 10.1002/eqe.3910

[11] Y.P. Oktiovan, L. Davis, R. Wilson, A. Dell'Endice, A. Mehrotra, B. Pulatsu, D. Malomo, Simplified Micro-Modeling of a Masonry Cross-Vault for Seismic Assessment Using the Distinct Element Method. *International Journal of Architectural Heritage*, 1-34, 2023. DOI: 10.1080/15583058.2023.2277328.

[12] B. Pulatsu, E. Erdogmus, P.B. Lourenço, Comparison of in-plane and out-of-plane failure modes of masonry arch bridges using discontinuum analysis. *Engineering Structures*, 178, 24-36, 2019. DOI: 10.1016/j.engstruct.2018.10.016

[13] K. Meguro, H. Tagel-Din, Applied element method for structural analysis: theory and application for linear materials. *Structural Engineering / Earthquake Engineering*, 17(1), 21s-35s, 2000.

[14] N. Scattarreggia, A. Orgnoni, R. Pinho, M. Moratti, G.M. Calvi, Failure analysis of the impact of a falling object on a bridge deck. *Engineering Failure Analysis*, 148, 107229, 2023. DOI: 10.1016/j.engfailanal.2023.107229

[15] H. M. Salem, H. M. Helmy, Numerical investigation of collapse of the Minnesota I-35W bridge. *Engineering Structures*, 59, 635–645, 2014. https://doi.org/10.1016/J.ENGSTRUCT.2013.11.022.

[16] D. Malomo, R. Pinho, A. Penna, Simulating the shake table response of unreinforced masonry cavity wall structures tested to collapse or near-collapse conditions. *Earthquake Spectra*, 36(2), 554-578, 2020. doi:10.1177/8755293019891715

[17] D. Malomo, R. Pinho, A. Penna, Using the applied element method for modelling calcium silicate brick masonry subjected to in-plane cyclic loading *Earthquake Engineering & Structural Dynamics*,47(7), 1610-1630, 2018. doi:10.1002/eqe.3032

[18] D. Malomo, R. Pinho, A. Penna, Applied element modelling of the dynamic response of a full-scale clay brick masonry building specimen with flexible diaphragms. *International Journal of Architectural Heritage*, 14(10), 1484-1501, 2020. doi:10.1080/15583058.2019.1616004

[19] L. Davis, M. Cogliano, C. Casotto, G. Grecchi, S. Ozcebe, C. Tsioli, D. Malomo, Pragmatic seismic collapse meso-scale analysis of old Dutch masonry churches. *Earthquake*

Engineering & Structural Dynamics, 53, 622–645, 2024. https://doi.org/10.1002/eqe.4037

[20] V. Alecci, G. Misseri, L. Rovero, G. Stipo, M. De Stefano, L. Feo, R. Luciano, Experimental investigation on masonry arches strengthened with PBO-FRCM composite. *Composites Part B: Engineering*, **100**, 228-239, 2016. https://doi.org/10.1016/j.compositesb.2016.05.063.

[21] MAPEI s.p.a, PLANITOP INTONACO ARMATO, available at https://www.mapei.com/it/en/products-and-solutions/products/detail/planitop-intonaco-armato.

[22] Applied Science International - ASI. Extreme Loading for Structures (2021), Durham (NC), USA.